International Journal of Innovative
Computing, Information and Control
Volume **19**, Number **2**, April **2023**

ICIC International ©2023 ISSN 1349-4198
pp. **403–418**

FRICTION COMPENSATION OF ELECTRIC CONTROL VALVE BASED ON SLIDING MODE WITH IMPROVED VARIABLE RATE POWER REACHING LAW

Yuanlong Yue*, Xiaobo Bai and Xin Zuo

Department of Automation
College of Information Science and Engineering
China University of Petroleum-Beijing
No. 18, Fuxue Road, Changping District, Beijing 102249, P. R. China
2020211241@student.cup.edu.cn; zuox@cup.edu.cn
*Corresponding author: yueyuanlong@cup.edu.cn

Received August 2022; revised November 2022

Abstract. *In this paper, an improved variable rate power reaching law of sliding mode control strategy is proposed for the position control system of electric control valve, which can improve the rapidity and robustness of electric valve with friction. Firstly, a dynamic model of electric control valve with friction is developed for the control system. Secondly, an improved variable rate power reaching law is proposed to keep high tracking performance of electric control valve, which can dynamically adjust the convergence rate of position tracking. In order to improve the performance in steady-state regime, the boundary layer is applied to attenuate the chattering issue of sliding mode control output. Finally, the effectiveness of the proposed reaching law control strategy is justified by simulation study on electric control valve with friction. The simulation results show that the control strategy not only ensures the better steady-state and dynamic performance of the electric control valve system, but also a better anti-interference ability.*
Keywords: Electric control valve, Friction, Sliding mode, Variable rate power reaching law, Boundary layer

1. **Introduction.** Control valves are one of the most common automation devices, which are widely used in aerospace, hydraulic engineering, petrochemical industry, environmental protection and other pipeline transportation systems [1]. The structure of electric control valve is relatively simple, mainly composed of motor, mechanical transmission mechanism, valve stem and spool unit. And the motor is its core control component. Compared with pneumatic control valves, electric control valves have the advantages of more convenient energy acquisition, faster response, higher adjustment accuracy, and greater output torque [2]. Especially in scenarios where there are high requirements for valve control accuracy, electric control valves have great advantages.

Friction is prevalent in nature and occurs in almost every mechanical device with moving parts [3,4]. Friction is highly nonlinear and may not only result in poor tracking accuracy, large steady state errors [5], dead zone and poor control performance, but also lead to slip jump phenomenon, unwanted oscillation and excessive wear [6]. The nonlinearity of electric control valves is mainly attributed to the friction generated by the valve packing, which is formed of rings of composite materials acting as a dynamic seal between the valve stem and the material flowing through the valve [7]. According to statistics, about 20%-30% of the oscillations in control loops are caused by friction and hysteresis

DOI: 10.24507/ijicic.19.02.403

in control valves [8]. Therefore, reducing the effects of friction in electric control valves is an important way to improve control performance.

In order to reduce the adverse effects of friction in control valves, researchers have proposed many control strategies and compensation methods including PID control strategies [9,10], adaptive control [11,12], machine learning and neural network-based methods [13,14], state-observer-based compensating control [15,16], sliding mode variable structure control [17-20], and so forth. Sliding mode control (SMC) is mainly designed for nonlinear systems, with the characteristics of simple structure and excellent robustness. SMC can effectively overcome the nonlinear characteristics of friction and is insensitive to parameters indeterminacy of control system, unmodeled dynamics, and unknown external disturbances [21,22]. With respect to motor control of electric control valves, Utkin, one of the founders of variable structure control, and his collegues have amply discussed the design methods of variable structure control in DC motors, permanent magnet synchronous motors and induction motors in their work [23,24]. Therefore, SMC has great advantages in the control of electric control valves with nonlinear friction. However, due to the switching characteristics of SMC, the output of the sliding mode controller is superimposed with high-frequency oscillations, which is regarded as chattering phenomenon. Chattering may eventually damage the motor and the mechanical transmission mechanism [25].

Scholars have conducted a lot of researches to alleviate the chatting. Gao first proposed the reaching law method and summarized three classical reaching laws to improve the dynamic response performance of the system and to attenuate the chatting by adjusting the reaching law parameters [26]. However, the three classical reaching law methods still have some shortcomings, such as slow reaching rate. Therefore, a double power reaching law is proposed, which consists of two idempotence terms with the same form based on the power reaching law. By setting the coefficient value of two idempotence terms to adjust the speed of the reaching law, the convergence speed and the dynamic quality are improved [27]. An enhanced exponential reaching law is proposed where the idempotence term coefficient of the power reaching law takes a fractional form, and the denominator polynomial is used to improve the dynamic response of the control system and reduce the chattering [28]. A segmentation function design method is used to segment the power reaching law, and the parameters of each section are designed separately to ensure that the sliding mode control has a faster convergence speed and less chattering at different stages [29]. A fractional order reaching law is designed using fractional calculus to cope with the control system of the manipulator, and it can enhance the robustness and weaken the chattering phenomenon of the control system by setting a suitable calculus operator [30].

However, the reaching laws designed above are set with fewer parameters and used fixed parameter values, which can only regulate the convergence rate and suppress chattering within a limited range. In order to improve the above deficiencies, the state variables of the control system can be introduced into the expression of reaching law, that is, to construct a variable gain coefficient polynomial containing the state variables of the system, so that the convergence rate can be dynamic adjusted by the change of state variables. A faster convergence rate is achieved when the system state is far from the sliding mode surface, and smaller chattering when the system is close to the sliding mode surface [31,32].

However, for the control system with particularly high control accuracy requirements, it is necessary to further reduce the chattering and ensure fast convergence rate. In this paper, a sliding mode control method with variable speed power reaching law is innovatively proposed for the electric control system with friction. Particularly, by adding a global variable gain polynomial term to the power reaching law, and introducing a polynomial expression containing the state variables of control system into the exponent of the

power term, the dynamic characteristics and robustness of the control system are greatly improved. Based on the above method, this paper introduces the boundary layer method and sets the appropriate value of the boundary layer, so that the control performance can be guaranteed while the chattering can be further attenuated.

The main contributions of this paper are summarized as follows.

1) The composition and motion characteristics of electric control valve are comprehensively analyzed. Taking the nonlinearity into account in the electric control valve model, a dynamic model of electric control valve with friction is established. With a moderate number of parameters, the model can better reflect the real dynamic characteristics of the electric control valve. And it can be applied to general electric control valves, with universality and practicality.

2) A novel improved variable rate power reaching law sliding mode controller is proposed in this paper. By introducing the global gain and the state variables of the control system in the reaching law, the controller not only makes the dynamic response of the control system faster but also has better robustness. By combining the boundary layer method, the chattering of the sliding mode control is significantly weakened, and the control performance is guaranteed at the same time.

This paper is organized as follows. Section 2 presents the process model of an electric control valve. The improved variable rate power reaching law sliding mode control is proposed in Section 3. In Section 4, a numerical simulation is presented to illustrate the advantages of the proposed method, and the results are depicted and discussed. Finally, the conclusions are drawn in Section 5.

2. **Problem Statement.** In Figure 1, the structure of an electric control valve is presented. The symbols in the electric control valve are defined as in Table 1. The electric control valve mainly consists of permanent magnet DC motor, planetary gear box, mechanical transmission mechanism, valve seat, and valve stem. The DC motor provides the

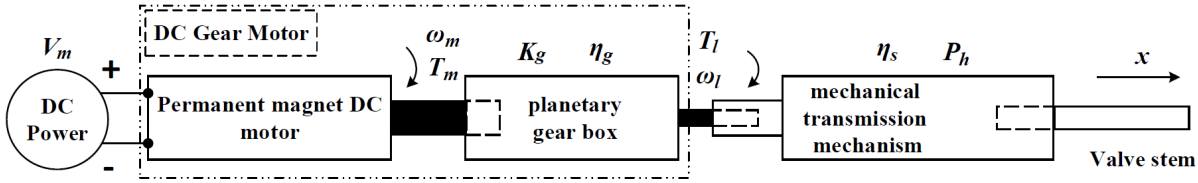

FIGURE 1. The composition of electric control valve

TABLE 1. The definitions of each symbol

Parameter	Description
V_m	The armature circuit voltage
ω_m	The motor shaft angular velocity
T_m	The torque constant
K_g	The reduction ratio of gear box
η_g	The gear box efficiency
T_l	The output torque of gear box
ω_l	The gear box shaft angular velocity
P_h	The lead of the screw
η_s	The screw efficiency
x	The relative stem position

power source for the valve stem, and the planetary gear box is used to reduce the angular velocity of the motor and increase the output torque. Then the mechanical transmission mechanism converts the rotary motion of the gear box into linear motion and drives the valve stem to make linear displacement, usually using a screw as the mechanism. A linear position sensor is also installed at the valve stem for real-time feedback on valve position.

There are many non-linearities, external disturbances and uncertainties in electric control valves, such as the backlash in the gear box, the friction of the valve stem seal packing, the voltage fluctuations in the DC power supply, the unbalanced fluid forces and changes in the parameters of the DC motor. These are generally ignored in the process of establishing the dynamic mathematical model of the electric control valve. However, the friction has a large impact on the electric control valve, which is difficult to ignore. In order to improve the accuracy of the model, the friction is taken into account in this paper when modelling the dynamic model of electric control valve. The dynamic modeling process is described in detail in the following.

According to Kirchhoff's voltage law, the DC motor' armature voltage is defined as

$$V_m = R_m i_m + L_m \frac{di_m}{dt} + e_m \tag{1}$$

where V_m, i_m, R_m, L_m, e_m represent the armature circuit voltage, the armature current, the armature resistance, the armature inductance and the motor back-emf voltage, respectively. The motor back-emf voltage $e_m = K_m \omega_m$, where K_m is the back-emf voltage constant, and ω_m is the motor shaft angular velocity. It should be noted that for typical DC servo motors, $L_m \ll R_m$, and therefore the inductance can be neglected. The armature current can be expressed as

$$i_m = \frac{V_m - K_m \omega_m}{R_m} \tag{2}$$

According to the Newton's second law, the gear box's equilibrium load can be expressed as

$$J_{eq} \dot{\omega}_l = T_l - T_L \tag{3}$$

where J_{eq} represents the rotational inertia of the gear box. ω_l represents the gear box shaft angular velocity. T_l represents the output torque of gear box. T_L represents the load torque. $\omega_l = \frac{\omega_m}{K_g}$, where K_g is the reduction ratio of gear box. $T_l = T_m \eta_g K_g$, where T_m represents the torque generated by DC motor, and η_g is the gear box efficiency. Consider the relationship between the DC motor torque T_m and the armature current i_m. The DC motor torque can be written as $T_m = K_T i_m$, where K_T represents the torque constant. (3) can be rewritten as

$$J_{eq} \dot{\omega}_l = K_T \eta_g K_g \frac{V_m - K_m K_g \omega_l}{R_m} - T_L \tag{4}$$

The dynamic equations of screw are defined as

$$\omega_l = \frac{2\pi \dot{x}}{P_h} \tag{5}$$

$$F = \frac{2\pi}{P_h} \eta_s T_L \tag{6}$$

where P_h is the lead of the screw, x is the relative stem position, F is the stem thrust, and η_s is the screw efficiency.

For the sliding stem, the force balance equation based on Newton's second law can be written as

$$m\ddot{x} = F - F_{friction} - F_{fluid} - F_{seat} \tag{7}$$

where m represents the mass of moving parts, $F_{friction}$ represents the friction force, F_{fluid} represents the force due to fluid pressure drop, and F_{seat} represents the extra force required the stem into the seat. F_{fluid} and F_{seat} can be negligible because they are two orders of magnitude smaller than other forces.

According to [3], the friction force can be modeled as

$$F_{friction} = \left[F_c + (F_s - F_c)e^{-\left(\frac{\dot{x}}{v_s}\right)^2}\right] sgn\left(\dot{x}\right) + F_V\dot{x} \tag{8}$$

where F_c is the Coulomb friction force, F_s is the static friction force, v_s is the Stribeck speed coefficient, and F_V is the viscous friction coefficient. The function $sgn()$ makes Equation (8) discontinue, but to design sliding mode controller, a smooth model is required. Therefore, sigmoid function tanh() is used to replace the sign function $sgn()$. Equation (8) can be rewritten as

$$F_{friction} = \left[F_c + (F_s - F_c)e^{-\left(\frac{\dot{x}}{v_s}\right)^2}\right] \tanh\left(\mu\dot{x}\right) + F_V\dot{x} \tag{9}$$

where μ is a positive constant which can adjust tanh() to approximate $sgn()$, as shown in Figure 2.

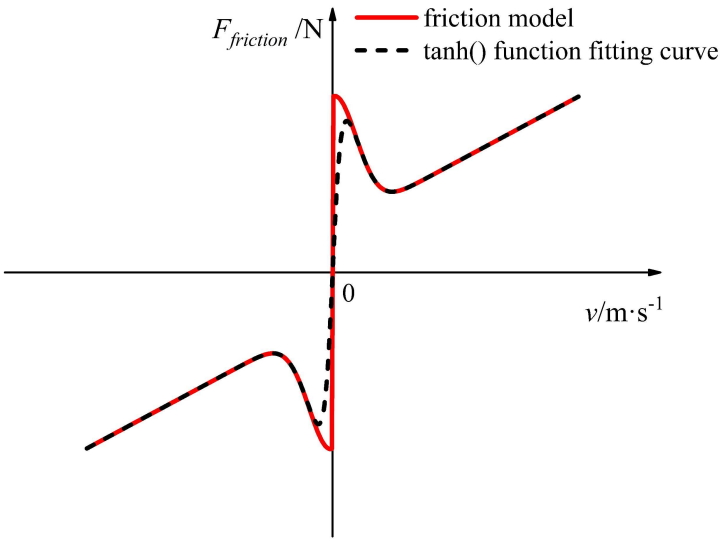

FIGURE 2. Stribeck friction model

According to Equations (4)-(7), the dynamic mathematical model of electric control valve is obtained as

$$J_{eq}\frac{2\pi\ddot{x}}{P_h} = \frac{K_T\eta_g K_g}{R_m}V_m - \frac{K_T\eta_g(K_g)^2K_m}{R_m}\frac{2\pi\dot{x}}{P_h} - \frac{P_h}{2\pi\eta_s}\left(m\ddot{x} + F_{friction}\right) \tag{10}$$

Let the variables $x_1 = x$ and $x_2 = \dot{x}$ be the system states, where $\dot{x}$ is the speed of stem. The space model of electric control valve with friction can be expressed as

$$\begin{cases} \dot{x}_1 = x_2 \\ \dot{x}_2 = \dfrac{1}{M}\left[\dfrac{K_T\eta_g K_g}{R_m}V_m - \dfrac{2\pi K_T\eta_g(K_g)^2K_m}{R_m P_h}x_2 - \dfrac{P_h}{2\pi\eta_s}F_{friction}\right] \end{cases} \tag{11}$$

where $M = \frac{J_{eq}\eta_s(2\pi)^2 + P_h^2 m}{2\pi\eta_s P_h}$, V_m is the sliding mode control input, and $y = x_1$ is the system output.

3. **Sliding Mode Controller Design.** For the model (11), the position tracking error of electric control valve is defined as $e = y - y_d = x_1 - y_d$, where y_d is the position setting value, and then $\dot{e} = x_2 - \dot{y}_d$.

The sliding surface is selected as

$$s = \dot{e} + Ce \tag{12}$$

where C is a strictly positive constant.

Differentiating the sliding surface, we have

$$\dot{s} = \ddot{e} + C\dot{e} \tag{13}$$

Substituting position tracking error e and its first-order derivative $\dot{e}$ into (13) obtains

$$\dot{s} = \dot{x}_2 - \ddot{y}_d + C\left(x_2 - \dot{y}_d\right) \tag{14}$$

Combining (11) and (14), the first-order derivative of sliding surface yields as

$$\dot{s} = \frac{1}{M}\left[\frac{K_T\eta_g K_g}{R_m}V_m - \frac{2\pi K_T\eta_g (K_g)^2 K_m}{R_m P_h}x_2 - \frac{P_h}{2\pi\eta_s}F_{friction}\right] + C\left(x_2 - \dot{y}_d\right) \tag{15}$$

3.1. **SMC design with improved variable rate power reaching law.** The traditional sliding mode control does not know the sliding process, and can lead to a high control activity, known as chattering. To gain a better control performance, the sliding mode control can use the reaching law strategy.

Mozayan et al. [28] proposed an enhanced exponential reaching law (EERL)

$$\begin{cases} \dot{s} = -k_1 s - \dfrac{k_2}{N(s)}|s|^{\lambda} sgn(s) \\ N(s) = \delta + (1-\delta)e^{-\gamma|s|^p} \end{cases} \tag{16}$$

where $k_1 > 0$, $k_2 > 0$, $0 < \lambda < 1$, $0 < \delta < 1$, $\gamma > 0$, $p = 1$.

If the initial value of s is large, the value of $N(s)$ converges to δ, EERL is $-k_1 s - \frac{k_2}{\delta}|s|^{\sigma} sgn(s)$, which is faster than conventional power reaching law $-k_1 s - k_2|s|^{\sigma} sgn(s)$. When s converges to sliding surface, the value of $N(s)$ converges to 1, and EERL is equivalent to the conventional power reaching law.

EERL can bring a fast convergence rate and reduce chattering, but the dynamic performance of electric control valve needs to be faster and in the steady state it is necessary to avoid stem chattering in order to prolong the valve life. To solve above mentioned issues, an improved variable rate power reaching law (VRPRL) is proposed with the following expression

$$\begin{cases} \dot{s} = \dfrac{1}{N(s)}\left[-k_1 s - k_2|s|^{\sigma(x_2)} sgn(s)\right] \\ N(s) = \delta + (1-\delta)e^{-\gamma|s|^p} \\ \sigma(x_2) = \alpha + (\lambda - \alpha)e^{-\beta|x_2|} \end{cases} \tag{17}$$

where $k_1 > 0$, $k_2 > 0$, $0 < \lambda < 1$, $0 < \delta < 1$, $\gamma > 0$, $p > 0$, $\alpha > \lambda$, $\beta > 0$.

As shown in Equation (17), the VRPRL introduces a global variable gain $N(s)$, relative to the EERL. If the initial s is large, the value of $N(s)$ converges to δ, and then the VRPRL converges to $\frac{1}{\delta}\left[-k_1 s - k_2|s|^{\sigma(x_2)} sgn(s)\right]$, which is faster than EERL under the same parameters. This means that the dynamic response is faster than EERL method. When s converges to sliding surface, the value of $N(s)$ converges to 1, and the variable rate power reaching law is equivalent to the conventional power reaching law.

The VRPRL also introduces the speed of stem x_2 in the exponential term of $|s|$ to control the convergence rate of s.

At the initial moment of the control system, $x_2 = 0$, $\sigma(x_2) = \lambda$, as x_2 increases, the value of $\sigma(x_2)$ increases and then reaches its maximum value. During this period, $k_2|s|^{\sigma(x_2)} > k_2|s|^{\lambda}$, VRPRL is faster than EERL, under the same parameters. In the middle and later stages of the dynamic response, $|x_2|$ gradually decreases and eventually converges to 0, $\sigma(x_2)$ decreases and converges to λ, at the same time. Introducing x_2 can dynamically adjust the reaching speed.

According to the above analysis, the innovative introduction of the global variable gain $N(s)$ and stem speed x_2 improves the dynamic response performance from two aspects. On the one hand, the global variable gain $N(s)$ enables the system to obtain a faster reaching rate than EERL method; on the other hand, the changing value of x_2 can accelerate the dynamic response rate in the initial stage and has smooth transition in the later stage. This is precisely the difference between VRPRL method and EERL method.

Finally, substituting the variable rate power reaching law (17) into Equation (15), the sliding mode control law u is obtained

$$u = \frac{R_m}{K_T \eta_g K_g} \left\{ \frac{M}{N(s)} \left[-k_1 s - k_2 |s|^{\sigma(x_2)} sgn(s) \right] + \frac{2\pi K_T \eta_g (K_g)^2 K_m}{R_m P_h} x_2 + \frac{P_h}{2\pi \eta_s} F_{friction} - C\left(x_2 - \dot{y}_d\right) \right\} \tag{18}$$

Lyapunov stability theory is an important tool for control system analysis and design. The system stability analysis is performed by introducing Lyapunov equation.

Theorem 3.1. *Under the effect of the variable rate power reaching law (17), the control system will converge to the equilibrium point $s = 0$.*

Proof: Construct the Lyapunov function as

$$V = \frac{1}{2} s^2 \tag{19}$$

Differentiating the sliding surface and substituting Equation (17) yields

$$\dot{V} = s\dot{s} = \frac{1}{N(s)} \left[-k_1 s^2 - k_2 |s|^{\sigma(x_2)+1} \right] \tag{20}$$

Obviously, $\dot{V} \leq 0$, and there is $\dot{V} = 0$, if and only if $s = 0$. Therefore, the system is asymptotically stable.

Remark 3.1. *The variable rate power reaching law can let the sliding mode function s reach the sliding surface $s = 0$, i.e., the control system output can track the setting value.*

3.2. **Boundary layer design.** To further improve the steady-state performance and reduce the chattering of the control system output, this paper uses the boundary layer combined with the reaching law sliding mode control.

The boundary layer uses the saturation function $sat()$ instead of the sign function $sgn()$ in the sliding mode control law, and the saturation function is shown in Equation (21). According to the expression of the saturation function, the normal sliding mode control is used outside the boundary layer, while the continuous state feedback control is used inside the boundary layer. This method is relatively simple and easy to implement.

If the boundary layer is too small, it will make the control gain too large to enhance the chattering although the control effect can be excellent. If the boundary layer is too large, the control effect becomes weak, and the dynamic performance and robustness of the control system will be adversely affected [24]. Therefore, it is necessary to pay

attention to the setting of the boundary layer to balance the relationship between control performance and the weakening of the chattering to obtain desired performance.

$$sat(s) = \begin{cases} sgn(s) & |s| > \Delta \\ s/\Delta & |s| \leq \Delta \end{cases} \tag{21}$$

4. **Simulation Results.** This section validates the effectiveness of the proposed SMC algorithm in the electric control valve with friction by simulation. The parameters of the DC gear motor and screw, produced by DONGZHENG MOTOR and Nanjing spring letter automation equipment company respectively, are shown in Table 2. The friction parameters are shown in Table 3. By conducting simulation experiments with these parameters, taking account of the limitation of DC voltage amplitude and the constraint of maximum output speed of the gear box, finally the setting of the values of reaching laws is obtained, shown in Table 4, so that the simulation results are close to the actual operation and more convincing. The classical power reaching law, the enhanced exponential

Table 2. The parameters of planetary gear motor and ball screw

Parameter	Description	Value
R_m	The armature resistance/(Ω)	4.5
K_m	The back-emf voltage constant	8.007×10^{-3}
K_T	The torque constant	7.67×10^{-2}
J_{eq}	The rotational inertia of the gear box/(kg.m^2)	37.04
K_g	The reduction ratio of gear box	422
η_g	The gear box efficiency	0.72
P_h	The lead of the screw/(m)	0.005
η_s	The screw efficiency	0.78

Table 3. The parameters of Stribeck friction

Parameter	Description	Value
m	Mass of valve stem and plug/(kg)	1.6
F_c	Coulomb friction/(N)	684
F_s	Striction friction/(N)	773
F_V	Viscous friction coefficient	2.32×10^4
v_s	Stribeck velocity/(m/s)	2.54×10^{-4}
μ	tanh() coefficient	10000

Table 4. The values of reaching laws

Parameter	(a)	(b)	(c)
k_1	0.1	0.1	0.1
k_2	0.016	0.016	0.016
λ	0.07	0.07	0.07
α	–	–	1.5
β	–	–	5
δ	–	0.01	0.01
γ	–	1	1
p	–	0.1	0.1

reaching law, and the variable rate power reaching law are respectively simulated and the results are compared with each other.

(a) The classical power reaching law (PRL)

$$\dot{s} = -k_1 s - \frac{k_2}{N(s)}|s|^{\lambda} sgn(s) \tag{22}$$

(b) The enhanced exponential reaching law (EERL)

$$\begin{cases} \dot{s} = -k_1 s - \dfrac{k_2}{N(s)}|s|^{\lambda} sgn(s) \\ N(s) = \delta + (1-\delta)e^{-\gamma|s|^p} \end{cases} \tag{23}$$

(c) The improved variable rate power reaching law (VRPRL)

$$\begin{cases} \dot{s} = \dfrac{1}{N(s)}[-k_1 s - k_2|s|^{\sigma(x_2)} sgn(s)] \\ N(s) = \delta + (1-\delta)e^{-\gamma|s|^p} \\ \sigma(x_2) = \alpha + (\lambda - \alpha)e^{-\beta|x_2|} \end{cases} \tag{24}$$

The reaching laws (22) and (23) are put into Equation (15) to obtain the sliding mode control laws, respectively. The initial states of the control system simulation are $y = 0$, $x_2 = 0$, the valve stem travel range is from 0 to 0.1 m, the parameter of sliding mode function (12) $C = 3.933$, and the stem setpoint is 20% of the stem travel range.

Figure 3 to Figure 5 show the simulation results of the system output tracking the valve displacement setting under different reaching laws without introducing boundary layer. Figure 3 shows the comparison of the position tracking result under the sliding mode control with different reaching laws. As is exemplified in Figure 3, the sliding mode control can effectively overcome the friction of the electric control valve. In the dynamic response process, the valve position output converges the slowest under the reaching law (a). Relatively, the reaching law (b) converges faster, and the reaching law (c) has the fastest dynamic response. From Figure 4, it can be seen that the error convergence rate of the reaching law (c) is faster than the other two reaching law methods. the PRL (a) has the slowest dynamic response and the VRPRL (c) has the fastest dynamic response. From Figure 4, it can be seen that the error convergence rate of the VRPRL (c) is the fastest among these three reaching law methods. Figure 5 shows the variation curves of s with

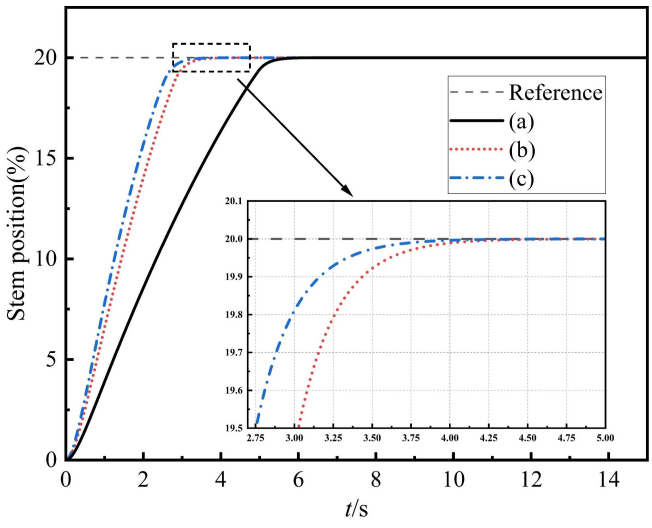

FIGURE 3. The position tracking result with different reaching laws

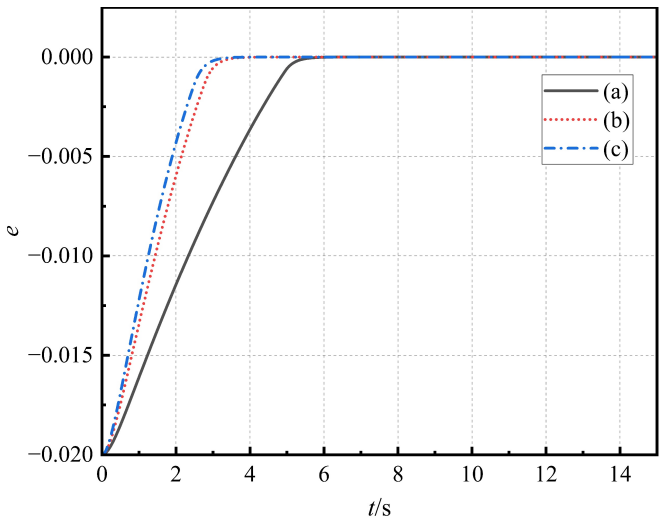

FIGURE 4. The position tracking error

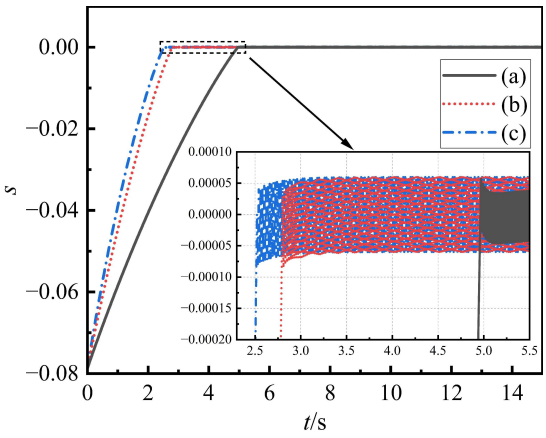

FIGURE 5. The convergence of s with different reaching laws

different reaching laws. From comparison of the s convergence in Figure 5, the VRPRL (c) can make the sliding mode variable s converge to the sliding surface faster than the others, so that the tracking error of the electric control valve also has a faster convergence speed. And the chattering still exists with three reaching laws, but the amplitude of chattering is very small, and the value of $|s|$ is less than 10^{-4} as can be seen in Figure 5.

The sliding mode control method based on the VRPRL (c) generates small-amplitude chattering. Considering that chattering may cause hazards such as high-frequency unmodeled dynamics of the control system, the boundary layer method is used to further reduce chattering. In the simulation experiments using the boundary layer method, the sign function $sgn()$ in the reaching law (a), (b), and (c) is replaced by the saturation function $sat()$, and the model parameters and friction parameters of the simulation remain unchanged. The stem setpoint is 20% of the stem travel range, and the boundary layer $\Delta = 0.001$. The simulation result is shown in Figure 6. Figure 6 shows the variation trend of each reaching law after adding the boundary layer. It can be seen that the chattering is substantially weakened after adding the boundary layer and the VRPRL (c) still has the fastest dynamic response. At the same magnification as in Figure 5, the chattering phenomenon can no longer be observed by using the boundary layer method, indicating that

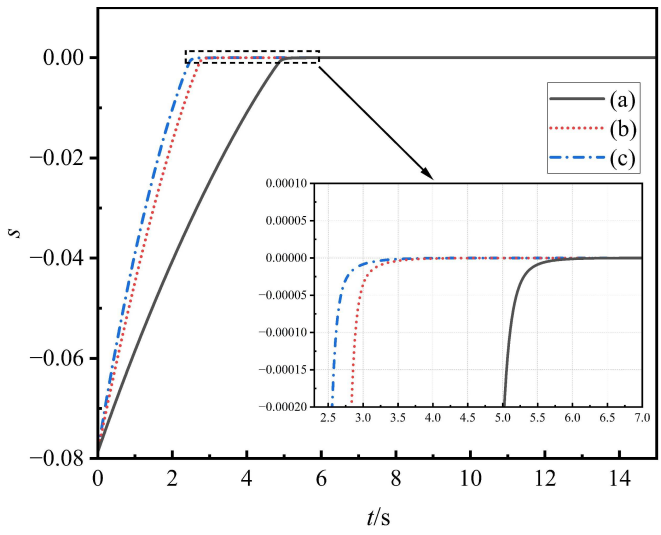

FIGURE 6. The convergence of s with boundary layer

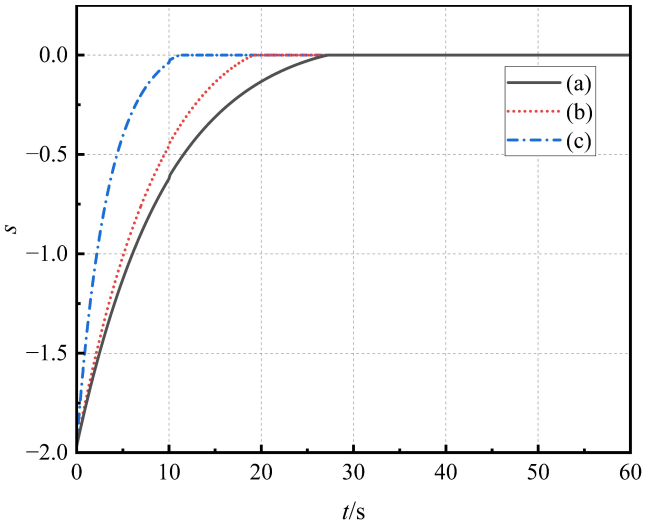

FIGURE 7. The convergence of s when the $|s| > 1$

the reaching law sliding mode control combined with the boundary layer has a stronger inhibitory effect on chattering.

Therefore, the superiority of VRPRL (c) sliding mode control for the dynamic response is verified in the simulation experiment, regardless of whether it contains a boundary layer or not.

To comprehensively analyze the validity of the method proposed in this paper, the initialization is set $|s| > 1$, and the convergence of s for each reaching law sliding mode method is compared. The dynamic mathematical model of electric control valve and reaching law sliding mode control parameters remain unchanged, and the condition of $|s| > 1$ is satisfied by changing the setpoint of the control system. From the simulation results shown in Figure 7, it can be seen that when the initial value of s is about -2, the s convergence speed of the VRPRL (c) is larger than that of the other two methods (a) and (b), as a result the convergence time of this method to the equilibrium state is significantly shorter. This indicates that the s converges faster with the variable rate power reaching law when $|s| > 1$, which ensures the faster valve position tracking. Therefore, compared

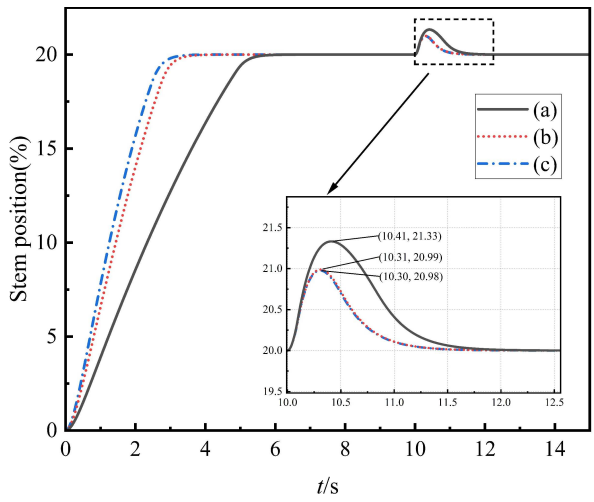

FIGURE 8. The position tracking result with boundary layer under disturbance

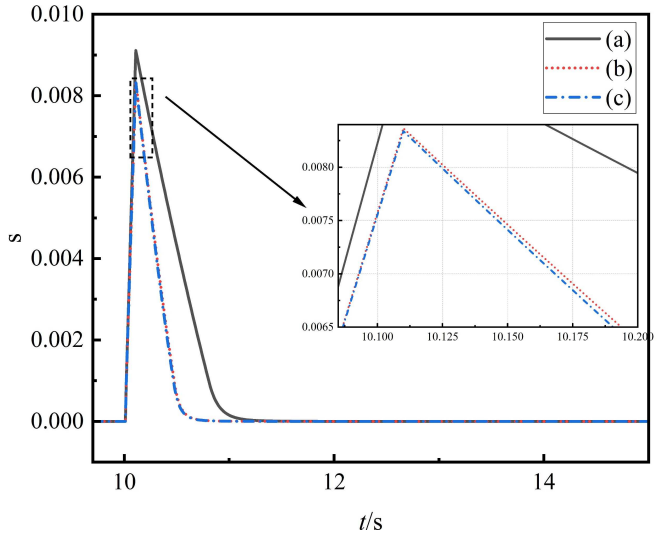

FIGURE 9. The convergence of s with boundary layer under disturbance

with methods (a) and methods (b), the VRPRL law (c) still ensures that the control valve has the fastest dynamic response, when s is far away from the sliding surface.

In order to verify the robustness of the VRPRL (c) in the valve position control system, an external disturbance is applied to the control system at the steady-state output period for simulation. The setpoint of valve position and other parameters are kept unchanged, the external disturbance is applied at $t = 10$ s, and the magnitude of the disturbance is $d = 0.1$ m/s^2. Figures 8 and 9 show the response of different reaching law sliding mode control for disturbance rejection. It can be easily seen in Figure 8 that the maximum value of the valve output with the PRL (a) is 21.33%, which is 1.33% larger than the steady state value after adding the disturbance, and the maximum values of the valve output with the EERL (b) and VRPRL (c) are 20.99% and 20.98%, respectively. The methods (b) and (c) consume less time to return to the steady state. Figure 9 shows the variation of s for each reaching law under the effect of disturbance. From Figure 9, the s of the VRPRL (c) converges to the equilibrium state relatively faster and the PRL (a) converges relatively slower under the effect of the disturbance. Therefore, the VRPRL

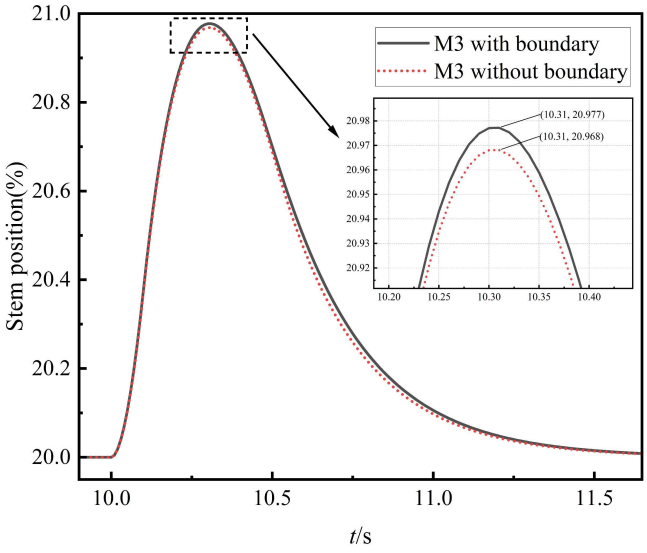

FIGURE 10. The effect of boundary layer on position tracking under disturbance

(c) has a better anti-disturbance ability and shorter recovery time, which ensures the robustness of the valve position control of the electric control valve.

The introduction of the boundary layer can further suppress the chattering, but it will reduce the control performance, which further weaken the robustness of the system. Therefore, it is necessary to analyze the robustness of the sliding mode control under the frame of VRPRL (c) both with and without the effect of boundary layer. Figure 10 shows the simulation results of the boundary layer on the disturbance rejection capability of the electric control valve position control system, in which the amplitude and introduction time of the disturbance remain unchanged. As can be seen in Figure 10, under the effect of disturbance, the valve tracking output of the VRPRL with boundary layer is larger than that without the boundary layer. It is verified that the introduction of the boundary layer impairs the control performance, but the difference between the two peak outputs is only 0.009%, indicating that the boundary layer setting is reasonable, which has little effect on the system, and ensures the robustness of the valve position control system with VRPRL (c) method.

In summary, the simulative experiment of the control of electric control valve with friction verifies that the variable rate power reaching law (VRPRL) sliding mode control has the fastest tracking speed, in comparison with the other two methods. It also verifies that the introduction of the boundary layer method can significantly weaken the chattering and improve the steady state output of the valve. The simulation with the external disturbance verifies that the variable rate power reaching law (VRPRL) sliding mode control has a better ability to suppress the disturbance. Finally, the simulation examines whether the inclusion of boundary layer has influence on valve position control, which verifies that the boundary layer value is set reasonably so that the valve position control system not only has excellent chattering reduction ability but also has a good robustness.

5. **Conclusions.** In this paper, a sliding mode control method based on the variable rate power reaching law has been proposed for the valve position control system. According to mechanism analysis, a dynamic model of electric control valve is established for simulation. A variable rate power reaching law method is proposed, and its asymptotic stability is proved theoretically. This method integrates the power reaching law and

the enhanced exponential reaching law, and introduces the system state variable. Compared with the power reaching law and the augmented exponential reaching law SMC, the variable rate power reaching law SMC makes the dynamic response of the system output faster. The boundary layer is introduced to improve the steady-state performance and alleviate the chattering of the traditional sliding mode control algorithm. By using simulations of an electric control valve model with friction, the control performance and robustness of variable rate power reaching law SMC and the other two reaching laws are compared. The simulation results show that the variable rate power reaching law SMC can effectively overcome the adverse effects of friction, and has faster dynamic response and better robustness.

This paper focuses on friction compensation of electric control valve based on sliding mode control strategy, so that the parameters of the electric control valve model, which actually vary in a small range, are set to constants. Meanwhile, the sliding mode control algorithm proposed in this paper is only simulated and has not been applied on the actual device. In order to make the research better, in the future, the time-varying characteristics of the parameters will be studied, the experimental platform will be set up and the control algorithm will be applied to the actual control valve for verification.

REFERENCES

[1] G. Ma, Z. Lin, Z. Zhu and Y. Fang, Effect of variable speed motion curve of electric actuator on ball valve performance and internal flow field, *Advances in Mechanical Engineering*, vol.13, no.6, DOI: 10.1177/16878140211028003, 2021.

[2] Y. Zhang and M. Cai, Overall life cycle comprehensive assessment of pneumatic and electric actuator, *Chinese Journal of Mechanical Engineering*, vol.27, no.3, pp.584-594, 2014.

[3] B. Armstrong-Hélouvry, P. Dupont and C. C. De Wit, A survey of models, analysis tools and compensation methods for the control of machines with friction, *Automatica*, vol.30, no.7, pp.1083-1138, 1994.

[4] C. C. De Wit, H. Olsson, K. J. Astrom and P. Lischinsky, A new model for control of systems with friction, *IEEE Trans. Automatic Control*, vol.40, no.3, pp.419-425, 1995.

[5] H. Olsson, K. J. Åström, C. C. De Wit, M. Gäfvert and P. Lischinsky, Friction models and friction compensation, *Eur. J. Control*, vol.4, no.3, pp.176-195, 1998.

[6] M. S. Choudhury, N. F. Thornhill and S. L. Shah, Modelling valve stiction, *Control Engineering Practice*, vol.13, no.5, pp.641-658, 2005.

[7] A. Kayihan and F. J. Doyle III, Friction compensation for a process control valve, *Control Engineering Practice*, vol.8, no.7, pp.799-812, 2000.

[8] B. C. Silva and C. Garcia, Comparison of stiction compensation methods applied to control valves, *Industrial & Engineering Chemistry Research*, vol.53, no.10, pp.3974-3984, 2014.

[9] R. B. di Capaci and C. Scali, An augmented PID control structure to compensate for valve stiction, *IFAC-PapersOnLine*, vol.51, no.4, pp.799-804, 2018.

[10] Y. Su, C. Zheng and P. Mercorelli, Velocity-free friction compensation for motion systems with actuator constraint, *Mechanical Systems and Signal Processing*, vol.148, 107132, DOI: 10.1016/j.ymssp.2020.107132, 2021.

[11] B. Rouzbeh, G. M. Bone, G. Ashby and E. Li, Design, implementation and control of an improved hybrid pneumatic-electric actuator for robot arms, *IEEE Access*, vol.7, pp.14699-14713, 2019.

[12] S. Wang and J. Na, Parameter estimation and adaptive control for servo mechanisms with friction compensation, *IEEE Trans. Industrial Informatics*, vol.16, no.11, pp.6816-6825, 2020.

[13] Z. Chu, G. Chen, J. Cui, S. Wang and F. Sun, Classifier-based approximator for friction compensation in high accelerated positioning system, *IEEE Trans. Industrial Electronics*, vol.68, no.5, pp.4090-4098, DOI: 10.1109/TIE.2020.2987268, 2021.

[14] R. Siraskar, Reinforcement learning for control of valves, *Machine Learning with Applications*, vol.4, 100030, DOI: 10.1016/j.mlwa.2021.100030, 2021.

[15] C. Ren, X. Li, X. Yang and S. Ma, Extended state observer-based sliding mode control of an omnidirectional mobile robot with friction compensation, *IEEE Trans. Industrial Electronics*, vol.66, no.12, pp.9480-9489, 2019.

[16] S. Thenozhi, A. C. Sánchez and J. Rodríguez-Reséndiz, A contraction theory-based tracking control design with friction identification and compensation, *IEEE Trans. Industrial Electronics*, vol.69, no.6, pp.6111-6120, 2021.
[17] M. C. Hidalgo and C. Garcia, Friction compensation in control valves: Nonlinear control and usual approaches, *Control Engineering Practice*, vol.58, pp.42-53, 2017.
[18] J. R. Baeza and C. Garcia, Friction compensation in pneumatic control valves through feedback linearization, *Journal of Control, Automation and Electrical Systems*, vol.29, no.3, pp.303-317, 2018.
[19] M. C. Hidalgo, C. Garcia, B. A. Angélico and E. A. Tannuri, Embedded sliding mode controller applied to control valves with high friction, *Journal of Control, Automation and Electrical Systems*, vol.30, no.5, pp.677-687, 2019.
[20] W. Ruan, Q. Dong, X. Zhang and Z. Li, Friction compensation control of electromechanical actuator based on neural network adaptive sliding mode, *Sensors*, vol.21, no.4, 1508, DOI: 10.3390/s21041508, 2021.
[21] Z. Liu, J. Yu, L. Zhao, Y. Ma, B. Xue and S. Cheng, Adaptive H_∞ sliding mode control for a class of uncertain Markovian jump systems with time-delay, *ICIC Express Letters*, vol.14, no.4, pp.319-327, 2020.
[22] X. Sun, J. Cao, G. Lei and J. Zhu, A composite sliding mode control for SPMSM drives based on a new hybrid reaching law with disturbance compensation, *IEEE Trans. Transportation Electrification*, vol.7, no.3, pp.1427-1436, 2021.
[23] V. Utkin, J. Guldner and J. Shi, *Sliding Mode Control in Electro-Mechanical Systems*, CRC Press Publishers, Boca Raton, 2017.
[24] J. K. Liu, *Sliding Mode Control Design and Matlab Simulation – The Basic Theoty and Design Method*, Tsinghua University Press Publishers, Beijing, 2019.
[25] H. Lin, K. Chen and R. Lin, Finite-time formation control of unmanned vehicles using nonlinear sliding mode control with disturbances, *International Journal of Innovative Computing, Information and Control*, vol.15, no.6, pp.2341-2353, 2019.
[26] W. B. Gao, *Theory and Design Method for Variable Sliding Mode Control*, Science Press Publishers, Beijing, 1996.
[27] H. X. Zhang, J. S. Fan, F. Meng and J. F. Huang, A new double power reaching law for sliding mode control, *Control and Decision*, vol.28, no.2, pp.289-293, 2013.
[28] S. M. Mozayan, M. Saad, H. Vahedi, H. Fortin-Blanchette and M. Soltani, Sliding mode control of PMSG wind turbine based on enhanced exponential reaching law, *IEEE Trans. Industrial Electronics*, vol.63, no.10, pp.6148-6159, 2016.
[29] X. Y. Yang, Y. R. Liao and S. Y. Ni, Rapid piecewise power reaching law of sliding mode control design and analysis, *Systems Engineering and Electronics*, vol.41, no.5, pp.1127-1132, 2019.
[30] X. Zhang, W. Lu, M. Su and W. Xu, Research on synchronous control strategy of robot arm based on cross-coupling control, *International Journal of Innovative Computing, Information and Control*, vol.16, no.6, pp.1987-2005, 2020.
[31] Y. Wang, Y. Zhu, X. Zhang, B. Tian, K. Wang and J. Liang, Anti-disturbance sliding mode-based deadbeat direct torque control for PMSM speed regulation system, *IEEE Trans. Transportation Electrification*, vol.7, no.4, pp.2705-2714, 2021.
[32] A. Goel and S. Mobayen, Adaptive nonsingular proportional-integral-derivative-type terminal sliding mode tracker based on rapid reaching law for nonlinear systems, *Journal of Vibration and Control*, vol.27, nos.23-24, pp.2669-2685, 2021.

Author Biography

Yuanlong Yue received the B.Sc. degree in automation and the Ph.D. degree in control science and engineering from China University of Petroleum-Beijing, China, in 2008 and 2014, respectively.

Dr. Yue is currently a senior engineer in automation at the College of Information Science and Engineering, China University of Petroleum-Beijing, China. His research interests include subsea production control systems design, subsea communication protocol, highly reliable imbedded system design, and multi-sensor data fusion. He is the author or coauthor of more than 20 refereed technical papers, and he is the holder of 6 patents in his areas of interest.

Xiaobo Bai obtained his Bachelor degree in automation from China University of Petroleum-Beijing, China in 2014 and he is currently working toward the M.Sc. degree in control science and engineering at China University of Petroleum-Beijing.

Mr. Bai's main interests and experience include the subsea production mechanical structure and control systems design, nonlinear compensation, DC motor control, valve structure and control design.

Xin Zuo received the B.Sc. degree from East China Petroleum Institute (now China University of Petroleum-Beijing), China, in 1984; he worked as the assistant at East China Petroleum Institute from September 1984 to August 1987; he received the Master degree in China University of Petroleum-Beijing, China, in 1990.

Prof. Zuo is currently a full-time professor at the College of Information Science and Engineering, China University of Petroleum-Beijing, China. He is a member of Expert Committee of China National Association for Automation in Petroleum and Chemical Industry. He is the author or coauthor of more than 110 refereed technical papers, and he is the holder of 20 patents in his areas of interest. His research interests include subsea production control systems design, subsea production reliability research, process control design and real-time optimization.